Carbohydrate Polymers 83 (2011) 1591–1597

Contents lists available at ScienceDirect

Carbohydrate Polymers

journal homepage: www.elsevier.com/locate/carbpol

Glycerol/starch/Na$^+$-montmorillonite nanocomposites: A XRD, FTIR, DSC and ^{1}H NMR study

Huihua Liu[a], Deeptangshu Chaudhary[a,*], Shin-ichi Yusa[b], Moses O. Tadé[a]

[a] Department of Chemical Engineering, Curtin University of Technology, Perth, Australia
[b] Department of Materials Science and Chemistry, University of Hyogo, Himeji, Japan

ARTICLE INFO

Article history:
Received 27 July 2010
Received in revised form 6 October 2010
Accepted 7 October 2010
Available online 15 October 2010

Key words:
Starch
Nanocomposite
Glycerol
XRD
Proton NMR

ABSTRACT

We studied the influence of glycerol/MMT loading on the nanocomposites morphology prepared from amylose starch biopolymer with various glycerol/MMT (Na$^+$-montmorillonite) concentrations. Samples were studied by X-ray diffraction (XRD), Fourier transform infrared spectroscopy (FTIR), differential scanning calorimetry (DSC) and proton nuclear magnetic resonance (^{1}H NMR) measurements. XRD results highlighted the impact of glycerol on the MMT exfoliation; with 15% glycerol imposed the largest inter-lamella spacing (*d*-spacing) value. Newly formed hydrogen bonds and the interaction among starch/glycerol/MMT were evidenced by peaks associated with –OH stretching located at 3300 cm^{-1} and 999 cm^{-1} from the FTIR spectra. DSC measurements revealed that glass transition temperature (T_g) decreased with increasing glycerol content. MMT also lowered the crystallization temperature (T_m) and suppressed the overall sample crystallinity. Proton NMR spectra obtained at 25 °C and 70 °C from samples containing only starch and glycerol provided important clues for explaining the starch and glycerol interaction.

1. Introduction

The wide application of biodegradable polymers in environmental friendly packaging and biomedical materials has seen increased attention by numerous researchers in recent years (Avella et al., 2005; Cyras, Manfredi, Ton-That, & Vázquez, 2008). Starch is a natural polymer that is cheap and readily available; however, its high T_g and water sensitivity limits its utilization in flexible packaging area (Lee, Chen, & Hanna, 2008). Recent research focuses on incorporating layered silicates, especially Na$^+$-montmorillonite that could be used as the reinforcing phase due to the latter's very high aspect ratio (~100). Thus, with a very low loading of MMT (1–10%), the produced nanocomposites exhibit up to tenfold increase in mechanical, thermal, electrical and barrier properties (Xiong, Tang, Tang, & Zou, 2008). Three types of morphology can be observed in starch-based nanocomposites which depend on the content of the MMT and the processing conditions: (a) intercalated (small amount of polymer moves into the gallery spacing between the silicate platelets), (b) exfoliated (completely and uniformly dispersed in polymer matrix) and (c) a combination of intercalated and exfoliated (Namazi, Mosadegh, & Dadkhah, 2009). The core issue discussed in all nanocomposites preparation is the dispersion of nanofiller within the polymer matrix via different methods and extrusion remains the widely used technique due to its versatility and scale-up capabilities (Lee & Hanna, 2008).

The unique aspect of this work is the modification of the MMT using the plasticizer itself and then, the objective of the present work is to examine the combined effect of glycerol concentration and Na$^+$-montmorillonite loading in the structural, morphology, thermal properties of biodegradable high-amylose nanocomposite prepared by extrusion. Therefore, we focused on understanding the relationship between the ratio of plasticizer/MMT and the morphology/dispersion degree of the MMT within the nanocomposite.

2. Material and method

2.1. Material preparation

Amylose starch (75% amylose) was purchased from National Starch Company (New Jersey, USA); glycerol was obtained from Food Dept Ltd. (Melbourne, Australia); MMT was supplied by NichePlas Ltd. (Sydney, Australia). 10 samples were prepared at different ratio of MMT/glycerol content. Moisture content of dry starch was adjusted to 35% (contains corresponding amount of glycerol) using a twin rotor kitchen bench-top mixer and kept in sealed polyethylene bags for equilibrium. MMT was added to dry starch biopolymer together with glycerol and water after sonication for

* Corresponding author. Tel.: +61 892662522; fax: +61 892662681.
E-mail addresses: Huihua.liu@postgrad.curtin.edu.au (H. Liu), d.chaudhary@curtin.edu.au (D. Chaudhary), yusa@eng.u-hyogo.ac.jp (S.-i. Yusa), M.O.Tade@curtin.edu.au (M.O. Tadé).

0144-8617/$ – see front matter © 2010 Elsevier Ltd. All rights reserved.
doi:10.1016/j.carbpol.2010.10.018

30 min. The sample nomenclatures used in this work are listed in Table 1. Each sample was described with a label such as G105, where G referred to glycerol, number 1 indicated 1% MMT used; 05 referred to the amount of glycerol within the samples.

A lab-scale twin screw co-rotating (SHJ-20, JieYa, China) was used to prepare nanocomposite samples. There are six heating zones from the feeding copper to the die, namely, zone 1 to zone 5 and die temperature. The temperature profile applied in the present work was optimized by examining the gelatinization degree for the extrudate, determined as 9 °C/110 °C/125 °C/120 °C/90 °C/50 °C from the feeding copper to die. Food dye (as tracer) was added to determine the residual time between different samples and subsequently determined as 13 min. In order to obtain most representative sample for each formula, only samples that after 8 min was collected. As processed noodle-like samples were cut into small pellets and then subjected to 70 °C oven drying for 20 h. Powder samples were obtained from milled dried pellets in a powerful ring miller. Samples were vacuum sealed for further characterizations.

2.2. Nanocomposite characteristics

Transmission electron microscopy (TEM) was carried out on the samples with MMT to determine the extent of MMT dispersion. TEM was performed on ultrathin sections at JEM-2100 microscope (JEOL, Tokyo, Japan), operating at an accelerating voltage of 200 kV. Oven-dried sample was sectioned at room temperature with diamond knife at Leica Ultramicrotome (EM UC7, Tokyo, Japan). Obtained sections, 100 nm thinness, are sandwiched between two 400-mesh copper grids for observation. X-ray diffraction is an important method to quantify the intercalated/exfoliated morphology in MMT composites. XRD analysis of the prepared samples were performed in a Bruker Discover 8 diffractometer operating at 40 kV and 40 mA with Cu Kα radiation ($\alpha = 1.54$ Å) with a 2θ range from 3° to 35° at a scan rate of 0.5°/s. The basal spacing of the silicate layered, were determined from the Bragg's equation, $\lambda = 2d \sin\theta$ (where θ is the diffraction position and λ is the wavelength) (Kampeerapappun, Aht-ong, Pentrakoon, & Srikulkit, 2007). The Fourier transform infrared spectra (FTIR) of all the samples were recorded in PerkinElmer 400 spectrometer using standard accessories in the range of 4000 cm^{-1} to 515 cm^{-1} for 74 scans.

DSC measurement was performed on SEIKO 6200 (Tokyo, Japan). About 10 mg of dried ground samples were place in an aluminum sample sealed pan. Sample was heated from −50 °C to 250 °C at a heating rate of 5 °C/min, kept at 250 °C for 5 min followed by cooling down to 25 °C at 10 °C/min. The glass transition temperature (T_g) was taken as the inflection point of the increment of specific heat capacity. Melting temperature was obtained for analysis as well. Dry powder sample of starch nanocomposites were dissolved in DMSO-d_6, which is a popular solvent for starch-nanocomposite in solution NMR measurement and the treatment of a nanocomposite with DMSO-d_6 does not affect the structural characteristic for amylose biopolymer (Fournaris, Karakassides, Petridis, & Yiannakopoulou, 1999), before proceeding to NMR measurement. 0.1 g of powder sample was dissolved in 1 ml DMSO-d_6 with 10 min of stirring and then kept in oven for two days at 80 °C to completely solubilize of the nanocomposite, as per an earlier report (Schmitz, Dona, Castignolles, Gilbert, & Gaborieau, 2008). The interaction between the plasticizers and the amylose biopolymer could be studied with the NMR spectra. The NMR data was collected for 16 scans on Bruker 500 at 25 °C and 70 °C, respectively. The chemical shift scale was calibrated using the residual DMSO-d_6 signal at 2.549 ppm (Hoffman, Arzuan, Pemberton, Aserin, & Garti, 2008).

3. Result and discussion

3.1. XRD analysis

The TEM slides and the XRD pattern for nanocomposites are shown in Fig. 1(a). When compared to pristine MMT (d-spacing value of 11.7 Å), all biopolymer nanocomposite samples showed increased d-spacing values. The augment was different from various composites, which indicated the glycerol and amylose chain had intercalated into the layer of MMT and force apart the MMT platelets depending upon the plasticizer and MMT concentrations. This is attributed to the overall interaction between the hydrophilic amylose and glycerol plasticizer, which can facilitate the polymer to penetrate into the hydrophilic Na^+-MMT gallery spacing (Chiou

Table 1
Moisture content, d-spacing, crystallinity, glass-transition temperature and melting temperature for nanocomposites prepared and theoretical plasticizer molecular structures.

Sample ID	PS	G010	G020	G105	G115	G200	G210	G220	G305	G315
Nanoclay (%)		0			1			2		3
Glycerol (%)	0	10	20	5	15	0	10	20	5	15
Moisture (%)	2.22	4.17	2.65	2.79	1.97	6.39	3.31	2.02	4.74	3.15
Xc[a] (%)	9.39	3.93	4.53	11.39	9.62	15.14	9.28	8.08	10.1	6.86
T_g (°C)	49.5	40.7	40.3	44.94	43.5	39.53	46.7	44.8	43.2	39.5
T_m (°C)	126	134	124.8	122	131	125	129	130	116	127
d-Spacing (Å)	–	–	–	16.96	17.92	16.96	17.72	17.82	17.52	17.92
Δd (Å)	–	–	–	5.26	6.22	5.26	6.02	6.12	5.82	6.22

Molecular structure[b]

Glycerol

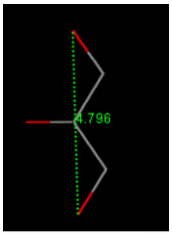

MS$_a$=4.796 Å

Maltodextrin

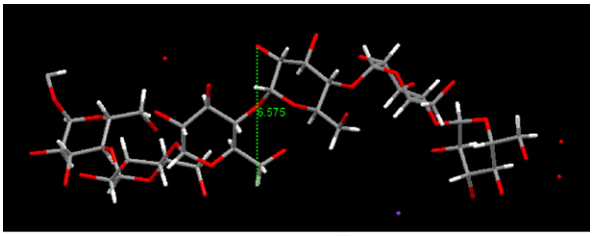

MS$_a$=6.575 Å

[a] Crystallinity calculated from the method described in Lopez-Rubio et al. (2008).
[b] Molecular structures are obtained from CCDC; colors: carbon atoms are gray, hydrogen-white, and oxygen-red).

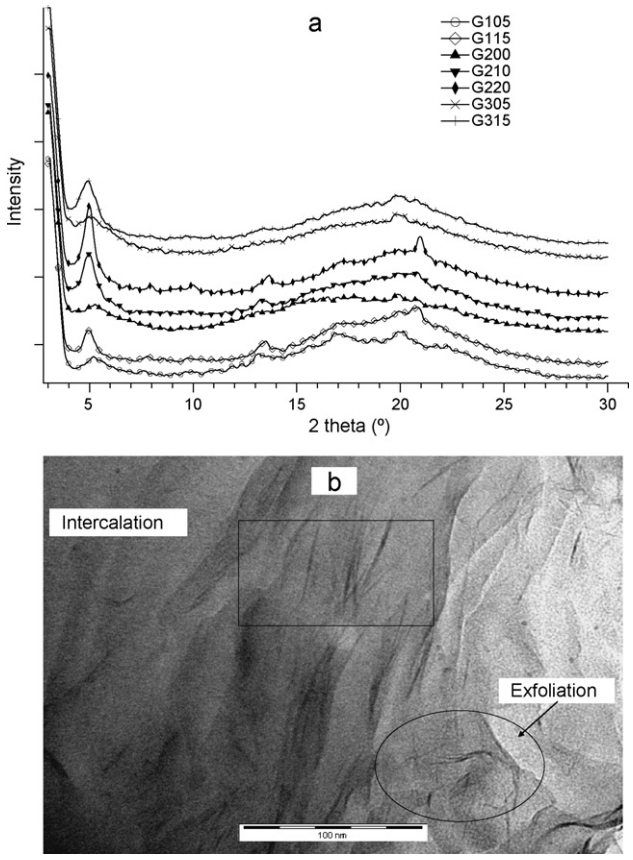

Fig. 1. (a) XRD diffractograms for nanocomposites and (b) TEM images for S305 (others not shown here).

et al., 2007). TEM images for representative sample (G305, others not shown here) clearly supported the statement that well intercalated composites with a higher 'gallery spacing' was achieved in all nanocomposites, Fig. 1(b). The analysis was carried out based on three groups of MMT loading, as shown in Table 1.

All the samples in Table 1 demonstrate significant augment in the MMT gallery spacing. We see that even without the glycerol addition, amylose molecules could be successfully intercalated into the 'gallery' of clay platelets by extrusion since the Δd values reasonably agree with the molecule size for glycerol/amylose fragments (Table 1). This is mainly attributed to hydrophilic interactions of pristine MMT particles, and the amylose/glycerol hydroxyl groups.

Pandey and Singh showed that mixing order influences MMT interaction in samples containing starch, MMT and glycerol, and they concluded that better dispersion of MMT is generated when starch and MMT are mixed without glycerol, because presence of glycerol strongly affects starch behavior (Pandey & Singh, 2004). In our preparation technique, MMT and glycerol was homogenized first, to allow glycerol to interact with the MMT gallery. It can be read from Table 1, that the MMT gallery spacing does increase with increasing the glycerol amount, e.g. the *d*-spacing value of G105 and G115 are 16.96 Å and 17.92 Å, respectively and this finding is not consistent with Choi et al.'s work (Chiou et al., 2007). The XRD investigations reveal that the (0 0 1) peak for clay appears to be sharper with increasing the glycerol amount (Fig. 1); which means the intercalation is limited and a possible reason for this behavior could be the higher glycerol concentration lead to a stronger glycerol–starch interaction (McGlashan & Halley, 2003) which limits the level of clay intercalation with clay–glycerol interactions.

From the XRD patterns, the peak broadening observed with 5% glycerol plasticizer indicates that the glycerol–MMT interaction is successful. X-ray peak broaden indicates that the crystal lattice has become imperfect, according to the theory of kinematical scattering, peak broadening is caused by either small crystal size or presence of large amount of lattice defects (Ungar, 2004). The peak intensity indicated the total scattering from each plane in the crystal structure and directly related to the distribution of MMT platelets structure (Connolly, 2003).

Further increase in glycerol enhanced the glycerol–starch interaction, which hinders the exfoliation of MMT platelets (as seen by comparing the XRD patterns for G105 (G305) and G115 (G315). Furthermore, increased starch–glycerol interaction would lead to increased intercalation of MMT platelets, and such agglomeration is reflected by the sharp XRD patterns for higher glycerol samples. It would be further supported by the DSC results in the following section where G105 (or G305) imposed lower melting temperature than G115 (or G315).

3.2. Moisture measurement and crystallinity

Starch equilibrium moisture measurements can indirectly indicate the strength and direction of interaction between the starch–glycerol and starch–MMT. In order to determined the absolutely moisture content of the prepared samples, samples were subjected to 20 h oven-dried to remove the free water within the sample. And then moisture meter (CA-100, Mitsubishi Chemical Corporation, Japan) was used to measure the absolutely moisture content, as shown in Table 1.

From Fig. 1, composites crystallinity were calculated on the basis of a peak fitting procedures that put forward by Amparo et al. (Lopez-Rubio, Flanagan, Gilbert, & Gidley, 2008) where they illustrated that this method, widely used for synthetic polymer, was better in reflecting the crystalline content of starch than the traditional two-phase model (Gernat, Radosta, Anger, & Damaschun, 1993; Gidley & Bociek, 1988). The method used here takes into account irregularities in crystals that are expected to co-exist in semi-crystalline materials and avoid the underestimation (two-phase method did not consider the diffuse scattering from non-perfect crystalline structure) of the crystalline content. Igor software package (Wavemetrics, Lake Oswego, Oregon) was used for curve fitting. The fitted coefficients are calculated based on minimized value of Chi-square using the Levenberg–Marquardt algorithm. Each fitting procedure was repeated eight times with different initial inputs to check for data reproducibility. As Amparo et al. (Lopez-Rubio et al., 2008) suggested, Gaussian shape had been confirmed to reflect the best fitting results even with poor initial guess, and the crystallinity for samples was calculated as, $Xc = \left(\sum_1^n ACi/At\right)$, where *ACi* is the area under each fitted crystalline peak with index *i* (please note that the first peak appear in nanocomposites samples had not been treated as crystalline peak since this peak was the characteristic peak for *d*-spacing of MMT) and *At* is the total area under the diffractogram pattern. The averaged crystallinity results were shown in Table 1.

Addition of glycerol significantly decreased the equilibrium moisture content; the moisture content for G200 and G210 was 6.393% and 3.308%, respectively. This decrease could be attributed to the strong interaction between glycerol and starch matrix where some water molecules were replaced by glycerol molecules. Due to relatively stronger starch–glycerol interaction, increasing the glycerol concentration decreased the moisture content regardless of the MMT amount. However, if glycerol concentration was fixed, it was found that the equilibrium moisture content was proportional to the MMT loading. The high moisture content from high-MMT samples was considered to be a result of greater resistance for mois-

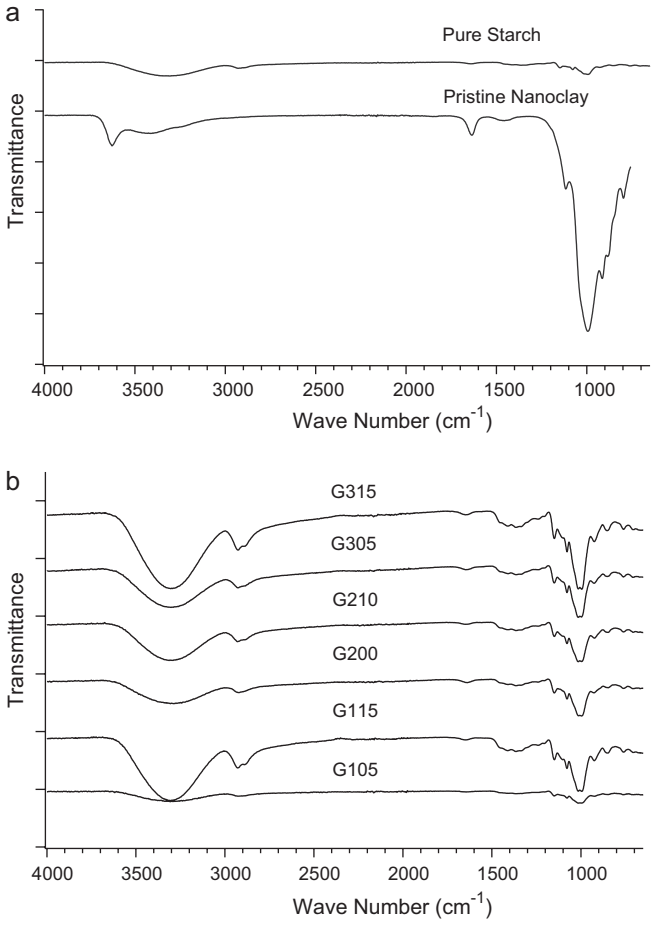

Fig. 2. FTIR spectra for (a) pure starch and pristine nanoclay (b) nanocomposite.

ture migration due to the well known tortuous pathway theory for water molecules. All extruded samples showed lower crystallinity value comparing to that of the native high-amylose starch (around 20%) (Cheetham & Tao, 1998). The nanocomposite crystallinity was dominated by the glycerol concentration; addition of glycerol dramatically decreased the crystallinity, e.g., crystallinity of G010 decreased from 9.39% to 3.93% after adding 10% glycerol to starch polymer. This trend was valid for samples with MMT, as seen in Table 1.

3.3. FTIR results

In Fig. 2(a), we note typical saccharide bands region located across of 1180 cm^{-1} to 953 cm^{-1} which is often considered as the vibration modes of C–C and C–O stretching and the bending mode of C–H bonds. These bands turned out to be the most intense in the IR-spectrum, as mentioned previously (Mousia, Farhat, Pearson, Chesters, & Mitchell, 2001). Bands at 3300 cm^{-1}, 1630 cm^{-1} and broader peaks centered around 2200 cm^{-1} were typical bands that associated with individual biopolymer components in addition to the contributions of the water absorptions (Souza & Andrade, 2002).

FTIR spectra for starch/MMT samples are shown in Fig. 2(b), and the shift of band 3627 cm^{-1}, from the free OH group of pristine MMT surface, to a lower frequency, 3302 cm^{-1} indicates the interaction between starch and MMT, and similar finding was reported in Field et al.'s work (Field, Sternhell, & Kalman, 2002). Comparing the spectrum of pristine MMT and the nanocomposite, the disappearance of the broader peak of H–OH stretching of water around 3234 cm^{-1} to 3486 cm^{-1} indicates the replacement of free water in the interlayer of pristine MMT by plasticizer/starch during the processing (Xu, Zhou, & Hanna, 2005) and this corroborates the XRD results that the *d*-spacing expanded to different extent in all nanocomposite samples.

The neat starch and composites present similar features in the FTIR spectral regions except the peaks related to OH stretching at 3290 cm^{-1}, 1630 cm^{-1} and 1046 cm^{-1}. Comparison based on samples with fixed MMT wt% and varying glycerol showed two bands at higher wavelength that exhibited size proportional to glycerol concentration, Fig. 3. It is important to understand the band changes associated with –OH groups, which suggested an increase in number of oscillation modes that could be attributed to the presence of new hydrogen bonding interactions (García, Ribba, Dufresne, Aranguren, & Goyanes, 2009). The presence of new and stronger hydrogen bonding could be concluded from the double peaks at 2919 cm^{-1} to 2887 cm^{-1} and 999 cm^{-1} to 992 cm^{-1} in nanocomposites samples when compared with pure starch (Ding, Ainsworth, Plunkett, Tucker, & Marson, 2006). The double peak of O–C stretching band at 999 cm^{-1} to 992 cm^{-1} results from bending both 'O' of C–O–H and 'O' of anhydrous glucose ring in starch molecules (Pushpadass, Marx, & Hanna, 2008). Therefore, it could be concluded that the extrusion of native starch to nanocomposite included the formation of hydrogen bonds and ternary interactions in starch/glycerol/MMT system.

3.4. Differential scanning calorimetry

The DSC thermograms of neat extruded starch, starch/glycerol composites and starch/glycerol/MMT nanocomposites exhibited glass transitions and crystallite melting endotherm typical of a semi-crystalline polymeric system. The T_g and T_m of all samples are presented in Table 1.

Neat extruded sample turned out to have the highest T_g value, 49.5 °C, similar to the results reported in Viguie et al.'s work that unplasticized starch had a unique transition around 50 °C (Viguié, Molina-Boisseau, & Dufresne, 2007), and T_g decreasing when increasing the glycerol concentration in the sample, 40.7 °C, 40.3 °C for 10% and 20% glycerol sample due to the plasticizing effect that improve the mobility of starch polymer chain (Pushpadass et al., 2008). The T_g for sample that incorporation of MMT, G200, decreased from 49.5 °C to 39.3 °C, this was inconsistent with the observations from Zeppa et al.'s work where they reported that an insignificant 3 °C change was found after incorporation of MMT (Zeppa, Gouanvé, & Espuche, 2009). Furthermore the decrease in T_m with addition of MMT, 108.92 °C and 125.95 °C for G200 and neat starch sample, respectively, was attributed to the reduced crystalline size and presence of crystal imperfections due to compatibility of the MMT with starch which suppressed the crystallization where the silicate platelet prevented the amylose chains to reorganise. However, it should be noted that the presence of MMT can allow smaller crystalline fractions to grow due to possible nucleating effect and this manifested as the larger crystallinity value in XRD measurements (Table 1). The above mentioned starch–glycerol interaction and the reduced mobility of the polymer can be further seen in samples with 10% glycerol which had significantly higher T_g value (from 40.7 °C (G010) to 46.7 °C (G210)), which strongly indicates polymer–plasticizer and polymer–MMT interactions.

Increasing the glycerol content further highlights the typical anti-plasticization to plasticization threshold, which have been discussed in one of our previous communications (Chaudhary, Adhikari, & Kasapis, 2010). The most interesting aspect was the suppression of 'anti-plasticization' behavior of starch–glycerol composites by the addition of MMT and causing an insignificant change in the T_g value (Chaudhary & Adhikari, 2009). Anti-plasticization is well known with lower glycerol concen-

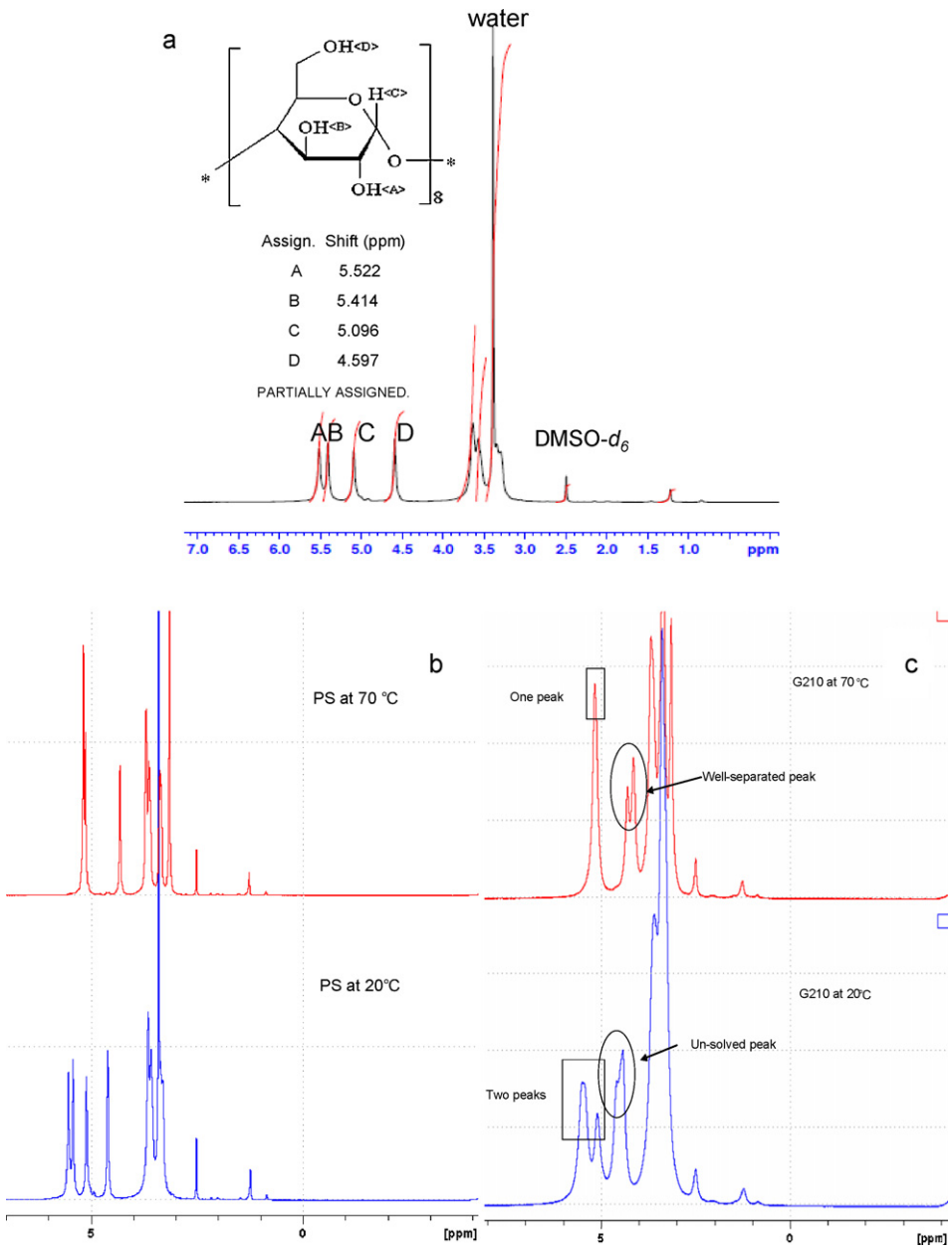

Fig. 3. ^{1}H NMR spectra in DMSO-d_6 for (a) extruded pure starch, (b) PS at 20 and 70 °C and (c) G210 at 20 and 70 °C.

tration because of strong starch–glycerol interaction that limits starch mobility and increases T_g. Therefore, when comparing samples with identical glycerol concentration at 5 wt%, increasing the amount of MMT (3% comparing to 1% MMT) slightly decreased the T_g value, and this could be explained by considering that the MMT was able to 'house' glycerol molecules such that the interaction between amylose chain and glycerol was reduced and this improved the chain mobility to some extent. The T_g values for G105 and G305 were 44.97 °C and 43.2 °C, respectively.

3.5. ^{1}H NMR

The spectrum of extruded pure starch is depicted in Fig. 3. The sharpest peaks, 3.410 ppm for PS, Fig. 3(b), observed in both spectra are from the OH of water in the sample. Four peaks located within the range of 5.6 ppm and 4.5 ppm could be assigned to corresponding to the OH groups from glucose unit of starch. Meanwhile, spectrum for sample which measured at 70 °C showed overall higher intensity and all peaks excepted DMSO-d_6 shifted to lower ppm when comparing to that of room temperature, Fig. 3(b). Different chemical environment usually leads to incompletely resolved peaks in ^{1}H NMR spectrum of polysaccharides because of the ring structure and anomeric oxygen atoms, hydrogen atoms linked to C-1(H1) are more de-shielded and consequently resonate at lower field strength (Casu, 1985). And another explanation stated this unresolved board peaks was arise from the overlapped phenomenon of resonance signal of starch/glycerol/water composite. However the un-solved peak was well separated when increasing the operating temperature, Fig. 3(c). The interaction between starch and glycerol was temperature dependant; and we can hypothesize that the interaction between starch/glycerol can be grouped into two main types, stable interactions and thermal dependant interactions, designated as resonance signal at 4.409 ppm and 4.484 ppm, respectively. However these two peaks were overlapped as the thermal energy increases as shown in spectrum from 70 °C measurement, Fig. 3(c).

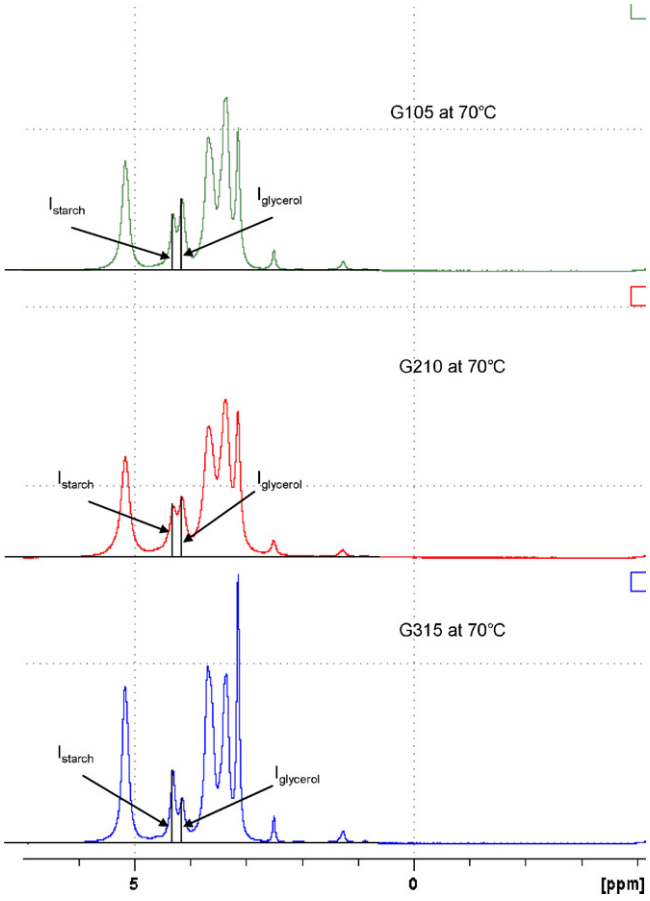

Fig. 4. ^{1}H NMR spectra for samples with different amount of plasticizer in DMSO-d_6 at 70 °C.

As the MMT cannot be solubilized in DMSO-d_6, different amount of precipitation are observed due to the MMT that has not interacted with the polymer structure. Strong interactions between the glycerol-modified MMT and the large polymer structure (Mol. Wt. > 100,000) allowed some of the MMT to stabilise in the solvent. Higher resolution spectra for nanocomposites were obtained. The peak intensity of NMR spectrum was directly related to the mobility of corresponding component. As illustrated in Fig. 4, peak located in 4.3 ppm and 4.1 ppm were assigned to starch and glycerol, respectively. When comparing the spectra from different amount of glycerol; it is interesting to note the ratio of $I_{glycerol}$ and I_{starch} increasing upon the glycerol concentration. However, $I_{glycerol}$ was observed to be smaller than I_{starch} in G105 indicating that the mobility of glycerol molecules was lower than that of starch chains. In other words, glycerol molecules were strongly 'locked' within the MMT network. And mobility of glycerol clearly increased when glycerol concentration increasing from 5% to 15%. Similar conclusion can be applied on the spectra from starch/glycerol samples, see Fig. 4. Unlike the addition of glycerol which resulted in some peak shift to a lower ppm; sample containing MMT have no effect on the peak position of starch, and same chemical shift for both G200 and pure starch was observed.

4. Conclusion

The influence of ratio of glycerol/MMT, varied from 1% to 20% and 1–3% for glycerol and MMT, respectively, on the characteristic of extruded starch nanocomposites was studied in the present work. Important conclusions can be drawn as follows:

1. Expansion of *d*-spacing, to different degrees, occurred in all MMT samples. Largest expansion occurred in 15% glycerol samples with a value of 17.926 Å which was believed to due to the interaction between plasticizer/plasticizer and plasticizer/starch taking the dominate place while the loading of plasticizer increasing.
2. Interactions between starch and MMT was concluded from the shift of band 3627 cm^{-1} (free OH group of MMT surface) to a lower frequency 3302 cm^{-1}. The double peak at 2919 cm^{-1} to 2887 cm^{-1} and 999 cm^{-1} to 992 cm^{-1} in extruded composites samples was compared with native starch and it shift confirmed the newly formed hydrogen bonding.
3. T_g values decreased when increasing glycerol concentrations, and this was attributed to the typical plasticization effect of glycerol. Incorporation of MMT caused the decrease of T_m due to the nucleating effect of MMT. MMT was also successful in balancing the starch–glycerol interaction to limit anti-plasticization.
4. ^{1}H NMR results showed the new formed peak at 4.409 ppm in G010, this peak was present as a result of the –OH group exchanges/interactions between high amylose chain and glycerol. Meanwhile NMR spectrum obtained at higher temperature (70 °C) imposed overall higher intensity than that from room temperature measurements, and this indicated that the interaction within the ternary system is temperature dependent.

Acknowledgments

The authors wish to thank Dr. Kyuya Nakagawa for his excellent technical assistance with the DSC. Acknowledge the internal funding from Curtin University of Technology. There is no potential conflict of interest between the researchers and this investigation does not bias any other investigation.

References

Avella, M., De Vlieger, J. J., Errico, M. E., Fischer, S., Vacca, P., & Volpe, M. G. (2005). Biodegradable starch/clay nanocomposite films for food packaging applications. *Food Chemistry*, *93*(3), 467–474.
Casu, B. (1985). Nuclear magnetic resonance studies of polysaccharide structure and interactions. *Polysaccharides, Topics in Structure and Morphology*, *1*.
Chaudhary, D., & Adhikari, B. (2009). Glass–rubber transition of plasticised starch biopolymer affected by relative humidity.
Chaudhary, D. S., Adhikari, B. P., & Kasapis, S. (2010). Glass transition behaviour of plasticized starch biopolymer system-a modified Gordon-Taylor approach. *Food Hydrocolloids*.
Cheetham, N. W. H., & Tao, L. (1998). Variation in crystalline type with amylose content in maize starch granules: An X-ray powder diffraction study. *Carbohydrate Polymers*, *36*(4), 277–284.
Chiou, B. S., Wood, D., Yee, E., Imam, S. H., Glenn, G. M., & Orts, W. J. (2007). Extruded starch-nanoclay nanocomposites: Effects of glycerol and nanoclay concentration. *Polymer Engineering and Science*, *47*(11), 1898–1904.
Connolly, J. R. (2003). Introduction quantitative X-ray diffraction methods.
Cyras, V. P., Manfredi, L. B., Ton-That, M. T., & Vázquez, A. (2008). Physical and mechanical properties of thermoplastic starch/montmorillonite nanocomposite films. *Carbohydrate Polymers*, *73*(1), 55–63.
Ding, Q. B., Ainsworth, P., Plunkett, A., Tucker, G., & Marson, H. (2006). The effect of extrusion conditions on the functional and physical properties of wheat-based expanded snacks. *Journal of Food Engineering*, *73*(2), 142–148.
Field, L. D., Sternhell, S., & Kalman, J. R. (2002). Organic structures from spectra. *Journal of Chemical Education*, *79*(11).
Fournaris, K. G., Karakassides, M. A., Petridis, D., & Yiannakopoulou, K. (1999). Clay-polyvinylpyridine nanocomposites. *Chemistry of Materials*, *11*(9), 2372–2381.
García, N. L., Ribba, L., Dufresne, A., Aranguren, M. I., & Goyanes, S. (2009). Physicomechanical properties of biodegradable starch nanocomposites. *Macromolecular Materials and Engineering*, *294*(3), 169–177.
Gernat, C., Radosta, S., Anger, H., & Damaschun, G. (1993). Crystalline parts of three different conformations detected in native and enzymatically degraded starches. *Starch-Stärke*, *45*(9), 309–314.
Gidley, M. J., & Bociek, S. M. (1988). Carbon-13 CP/MAS NMR studies of amylose inclusion complexes, cyclodextrins, and the amorphous phase of starch granules: Relationships between glycosidic linkage conformation and solid-state carbon-13 chemical shifts. *Journal of the American Chemical Society*, *110*(12), 3820–3829.
Hoffman, R. E., Arzuan, H., Pemberton, C., Aserin, A., & Garti, N. (2008). High-resolution NMR. *Journal of Magnetic Resonance*, *194*(2), 295–299.

Kampeerapappun, P., Aht-ong, D., Pentrakoon, D., & Srikulkit, K. (2007). Preparation of cassava starch/montmorillonite composite film. *Carbohydrate Polymers*, *67*(2), 155–163.

Lee, S. Y., Chen, H., & Hanna, M. A. (2008). Preparation and characterization of tapioca starch-poly (lactic acid) nanocomposite foams by melt intercalation based on clay type. *Industrial Crops and Products*, *28*(1), 95–106.

Lee, S. Y., & Hanna, M. A. (2008). Tapioca starch-poly (lactic acid)-Cloisite 30B nanocomposite foams. *Polymer Composites*, *30*(5), 665–672.

Lopez-Rubio, A., Flanagan, B. M., Gilbert, E. P., & Gidley, M. J. (2008). A novel approach for calculating starch crystallinity and its correlation with double helix content: A combined XRD and NMR study. *Biopolymers*, *89*(9), 761–768.

McGlashan, S. A., & Halley, P. J. (2003). Preparation and characterisation of biodegradable starch-based nanocomposite materials. *Polymer International*, *52*(11), 1767–1773.

Mousia, Z., Farhat, I. A., Pearson, M., Chesters, M. A., & Mitchell, J. R. (2001). FTIR microspectroscopy study of composition fluctuations in extruded amylopectin-gelatin blends. *Biopolymers*, *62*(4), 208–218.

Namazi, H., Mosadegh, M., & Dadkhah, A. (2009). New intercalated layer silicate nanocomposites based on synthesized starch-g-PCL prepared via solution intercalation and in situ polymerization methods: As a comparative study. *Carbohydrate Polymers*, *75*(4), 665–669.

Pandey, J. K., & Singh, R. P. (2004). Green nanocomposites from renewable resources: Effect of plasticizer on the structure and material properties of clay-filled starch. *Starch-Stärke*, *57*(1), 8–15.

Pushpadass, H. A., Marx, D. B., & Hanna, M. A. (2008). Effects of extrusion temperature and plasticizers on the physical and functional properties of starch films. *Starch-Stärke*, *60*(10), 527–538.

Schmitz, S., Dona, A. C., Castignolles, P., Gilbert, R. G., & Gaborieau, M. (2008). Assessment of the extent of starch dissolution in dimethyl sulfoxide by ^{1}H NMR spectroscopy. *Macromolecular Bioscience*, *9*(5), 506–514.

Souza, R. C. R., & Andrade, C. T. (2002). Investigation of the gelatinization and extrusion processes of corn starch. *Advances in Polymer Technology*, *21*(1), 17–24.

Ungar, T. (2004). Microstructural parameters from X-ray diffraction peak broadening. *Scripta Materialia*, *51*(8), 777–781.

Viguié, J., Molina-Boisseau, S., & Dufresne, A. (2007). Processing and characterization of waxy maize starch films plasticized by sorbitol and reinforced with starch nanocrystals. *Macromolecular Bioscience*, *7*(11), 1206–1216.

Xiong, H. G., Tang, S. W., Tang, H. L., & Zou, P. (2008). The structure and properties of a starch-based biodegradable film. *Carbohydrate Polymers*, *71*(2), 263–268.

Xu, Y., Zhou, J., & Hanna, M. A. (2005). Melt-intercalated starch acetate nanocomposite foams as affected by type of organoclay 1. *Cereal Chemistry*, *82*(1), 105–110.

Zeppa, C., Gouanvé, F., & Espuche, E. (2009). Effect of a plasticizer on the structure of biodegradable starch/clay nanocomposites: Thermal, water-sorption, and oxygen-barrier properties. *Journal of Applied Polymer Science*, *112*(4), 2044–2056.